

New solution for the high accuracy alignment of accelerator components

D. Caiazza, N. Catalan Lasheras, H. Mainaud Durand,* M. Modena, C. Sanz,
D. Tshilumba, V. Vlachakis, M. Wendt, and S. Zorzetti

CERN, CH-1211 Geneva, 23, Switzerland

(Received 29 March 2017; published 3 August 2017)

Several state-of-the-art metrology measurement methods have been investigated and combined for a fiducialization of accelerator components in the micrometric regime. The PACMAN project at CERN applied stretched-wire measurement methods to Compact Linear Collider quadrupole and cavity beam position monitor prototypes, to locate their magnetic, respectively, electromagnetic, axis using a dedicated test stand and to determine the position of the wire with respect to external alignment targets (fiducials) testing different methods, such as coordinate measuring machine measurements and microtriangulation. Further studies have been performed using a nanopositioning system, verifying the absolute accuracy and repeatability of the fiducialization method within a few micrometers.

DOI: [10.1103/PhysRevAccelBeams.20.083501](https://doi.org/10.1103/PhysRevAccelBeams.20.083501)

I. INTRODUCTION

Fiducialization is one of the key steps in the alignment of components for particle accelerators, such as magnets, accelerating structures, beam diagnostic devices, etc. [1]. It consists of determining the position of the internal reference axis of a given component with respect to external targets (fiducials) that are fixed on its external shape and remain visible during installation. The reference axis is defined in different ways depending on the function of the component; e.g., it is the magnetic center axis in the case of a quadrupole magnet or the electromagnetic symmetry axis for a beam position monitor (BPM) or an accelerating structure (AS)—in other words, a symmetry axis of the component that matches the nominal beam trajectory but not necessarily the mechanical symmetry axis. During the installation, the fiducials will be used to align the components to their theoretical position based on the tunnel general coordinate system, without requiring access to their reference axes.

At CERN (Geneva, Switzerland), a study for the next-generation e^+e^- linear collider for high energy physics experiments is underway. For this Compact Linear Collider (CLIC), the final beam alignment will be performed by means of beam-based measurements. However, a very precise prealignment of every component on a common girder is required: with an accuracy up to $10\ \mu\text{m}$ along a 200-m-long sliding window [2]. A first step of this prealignment is the precise fiducialization of each

component for which an accuracy of $\pm 5\ \mu\text{m}$ at 1σ is budgeted. The aim of the PACMAN project, a study on particle accelerator components' metrology and alignment to the nanometer scale, lies in the development of novel methods and tools, allowing the fiducialization of different types of accelerator components simultaneously within the environment of a 3D coordinate measuring machine (CMM). This project aims to improve the efficiency and accuracy of the process in view of the large number of components needed in the CLIC accelerator [3,4].

We use an assembly which consists of two critical CLIC main beam components: a 15 GHz cavity BPM and a quadrupole. A wire stretched through the component aperture is used to locate the reference axis of both components, a method which was performed previously at the TESLA Test Facility phase II (TTF2), now called FLASH [5]. In that case, the relative position between the BPM and quadrupole was analyzed based on electromagnetic, respectively, magnetic, characterization and stored for future reference. In our PACMAN project, thanks to the use of a CMM, we obtained absolute measurements of both components in a common metrological reference system (based on the same stretched wire). Furthermore, we also investigated the implementation of other means of portable metrology, namely, frequency scanning interferometry (FSI) and microtriangulation.

The central piece of hardware delivered by the project is called the Final PACMAN Alignment Bench (FPAB), a precision bench setup to characterize prototypes of the main accelerator components, utilizing stretched-wire measurements and advanced fiducialization methods. The bench integrates the measurement hardware and methods previously developed and tested on the individual assembly stands.

In Sec. II, we present the Final PACMAN Alignment Bench in detail, including the accelerator components to be analyzed, the measurement methods, and related technical

*Corresponding author.
helene.mainaud.durand@cern.ch

Published by the American Physical Society under the terms of the Creative Commons Attribution 4.0 International license. Further distribution of this work must maintain attribution to the author(s) and the published article's title, journal citation, and DOI.

systems and features of the bench. Section III describes the preparation, setup, and integration of the components to be analyzed on the FPAB. Section IV presents preliminary results of the measurements, and Sec. V discusses future perspectives of the project.

II. THE FINAL PACMAN ALIGNMENT BENCH

A. Prealignment requirements

As mentioned before, an accuracy up to $10\ \mu\text{m}$ will be needed for the prealignment of the CLIC main beam components. More specifically, along the main linac, the standard deviations of the transverse position of the BPM, quadrupole, and AS with respect to a straight line fit will have to be respectively 14, 17, and $14\ \mu\text{m}$. These values are the square root of the sum of the squared errors associated with the prealignment process, integrating the error of fiducialization, the error of position determination of the fiducials with respect to prealignment sensor interfaces, the prealignment sensor accuracy, the prealignment sensor linearity, and the stability and knowledge of the reference considered as a straight line (see Table I).

The last three steps have been validated successfully through a series of tests and dedicated mock-ups [1,2,6]. For the first two steps, only the mechanical fiducialization (determination of the mechanical axis of the components with respect to fiducials) was considered in the preliminary studies, plus the best results of fiducialization obtained at other facilities. At SLAC, using a combination of stretched-wire measurements for the quadrupole and CMM measurements, an accuracy of $25\ \mu\text{m}$ was reached for the fiducialization of the Linac Coherent Light Source components [7]. An accuracy of $12\ \mu\text{m}$ was reached for the fiducialization of the final focus test beam components using tooling plates [8]. In 2010, a literature review on fiducialization methods and initial alignment of components on girders had shown that the most accurate requirements concerned the SOLEIL synchrotron with an accuracy of $20\ \mu\text{m}$ in the horizontal and vertical initial alignment of the quadrupoles on the same girder [9]. The objectives of the FPAB are to carry out the measurements of

the first two steps at the same time and demonstrate that such a budget of errors is achievable.

B. Description and objectives of the Final PACMAN Alignment Bench

To achieve measurements of the highest accuracy and repeatability, the FPAB was located in the dedicated, temperature-stabilized measurement room of the CERN metrology laboratory, which hosts the Leitz Infinity CMM (MPEE = $0.3\ \mu\text{m} + L/1000$). This CMM has a maximum measurement range of $\sim 1.2\ \text{m}$, which represents the limit of the maximum physical length of the FPAB we can measure. Therefore, we focused this study on the measurement of an $\sim 0.6\ \text{m}$ long subassembly, consisting of a CLIC main beam quadrupole magnet with the attached cavity BPM. The two components are supported on a nanopositioning system. All components are equipped with fiducials, as shown in Fig. 1.

Such a bench will allow the validation of the concepts and tools developed to determine the magnetic and electrical axes of quadrupoles and BPM using a stretched wire. The measurements will be performed according to the process described hereafter. First, the wire will be placed at the magnetic axis of the quadrupole using the displacement stages. Its position will be measured by the CMM (or alternative solutions like microtriangulation), with respect to all the alignment targets, in the CMM coordinate system. Second, the wire will be placed at the electrical axis of the BPM using the displacement stages. Its position will be measured by the CMM (or alternative solutions) with respect to all the alignment targets in the CMM coordinate system. In two series of measurements, the fiducialization of the quadrupole and the fiducialization of the BPM will have been achieved at a micrometric accuracy, plus the determination of the relative position of the magnetic axis of the quadrupole with respect to the electrical axis of the BPM, also at a micrometric accuracy.

Our results will be extrapolated to the standard 2 m long CLIC accelerator module, which also holds the AS to be aligned on the same axis as the quadrupole-BPM assembly, demonstrating the required accuracy and resolution. However, because of the length limitation, the determination of the electromagnetic center axis of the rf structure had to be performed as a separate activity in our project [10] but could be implemented at a later stage as required.

The components of the FPAB are detailed in the next chapters.

C. The quadrupole magnet

The main beam quadrupole (MBQ) magnet to be integrated in the FPAB is a full-size, so-called type 1 prototype. The magnet design was developed and optimized during the past years as part of the CLIC R&D phase. The result is a compact, high-gradient magnet with minimum mass and dimensions.

TABLE I. Prealignment global budget of errors.

Prealignment steps	BPM, AS (μm)	Quadrupole (μm)
Fiducialization (reference axis vs fiducials)	5	10
Fiducials to prealignment sensor interface	5	5
Prealignment sensor accuracy	5	5
Prealignment sensor linearity	5	5
Stability, knowledge of the straight reference	10	10
GLOBAL ERROR BUDGET	14	17

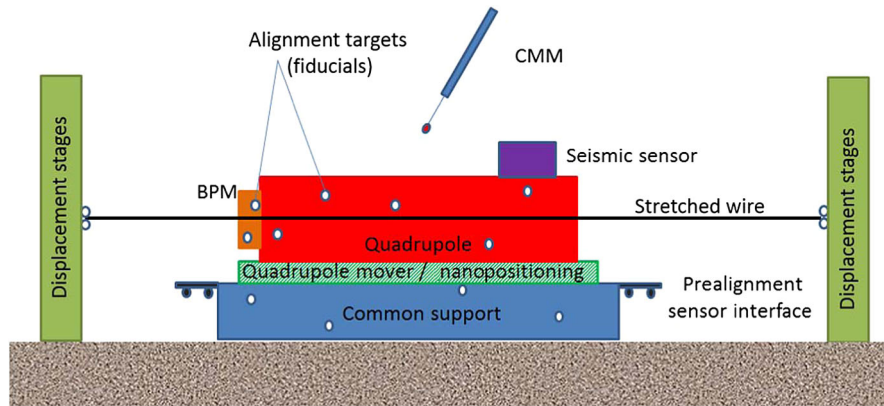


FIG. 1. The FPAB and its technical systems.

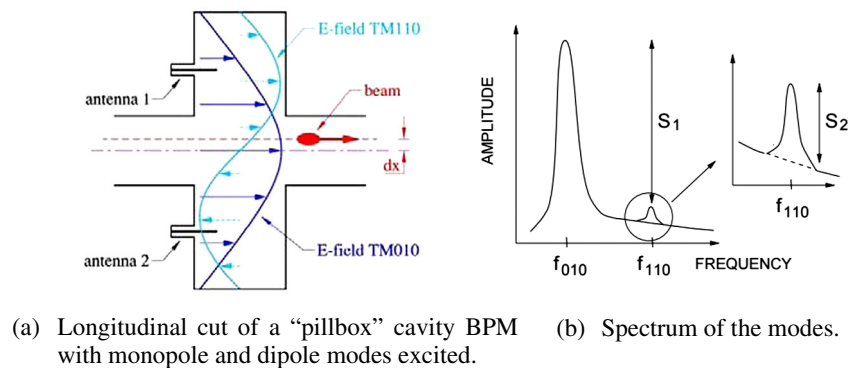


FIG. 2. Details of the modes excited in the position cavity.

The magnet has to be integrated into the crowded, 2 m long CLIC module. On top, the tight CLIC beam dynamics requirements can be fulfilled only with an active stabilization of the magnet by means of piezoactuators. This puts a limit on the mass of the magnet and imposes solid iron (not laminated) core quadrants as the structural choice to increase the stiffness. The additional advantage of this choice lies in the precision manufacturing of the pole tips utilizing a fine-grinding technique. After several iterations with European industry, a very satisfactory tolerance of $\pm 7 \mu\text{m}$ for the profiles of the iron poles was achieved [11].

A consequence of the compact magnet design is its operation close to the field saturation of the iron core under nominal conditions. Despite this fact, the magnetic stray field measured near the magnet is sufficiently low and has shown no major impact on the surrounding components and systems of the FPAB at a low excitation current of 4 A.

The magnetic axis of a quadrupole magnet is defined as the locus of points within its aperture where the magnetic flux density is zero. One way to determine it is to use a vibrating stretched wire, introduced in Sec. IV A.

D. The BPM

The BPM prototype used in the FPAB is a passive resonant cavity BPM, developed during the CLIC R&D phase and also installed in the CLIC Test Facility (CTF3/Califes). The design of the cavity BPM is based on the combination of a monopole mode (TM010) reference cavity and a dipole mode (TM110) position cavity. Both cavities operate at 15 GHz, a harmonic of the 1.5 GHz bunching frequency in CTF3. The dipole mode (position) cavity returns a signal proportional to the position and intensity coordinates of a bunched beam passing through the monitor, while the monopole mode (reference) cavity is used for normalizing that information to the beam intensity. The choice of this BPM type was driven by a high spatial and temporal resolution potential, less than 50 nm and 50 ns, respectively.

The fundamental mode of the position cavity is the monopole one TM010, excited at about 11 GHz, a frequency lower than that of the operating dipole mode (15 GHz). We are interested to utilize the beam excited first dipole eigenmode, indicated in Fig. 2(a), as it has an almost

linear dependency with the beam position for small beam displacements. To discriminate the dipole mode excited signal from the strong monopole mode signal, four lateral waveguides are added. They act as high pass filters, passing only signal frequencies $f > f_{010}$; see the illustration in Fig. 2(b) [12,13].

The BPM and quadrupole magnet are mounted together as a rigid assembly, enabling the measurement and steering of the beam on a trajectory with the minimum emittance dilution, which typically is close to the center of the quadrupole. The electrical center of the BPM is defined as the physical position in which the dipole mode is zero. In addition, the linear range of the position response signal of the BPM has to be determined, enabling a maximum measurement range of the BPM. For this reason, the cavity BPM needs first to be characterized by means of a prealignment procedure, to calibrate the BPM output signal after the BPM has been rigidly fixed to the quadrupole magnet. An accurate mechanical interface between the BPM and magnet was developed; it is described in Sec. III A.

E. The stretched-wire displacement system

The PACMAN stretched-wire system to localize the reference axis is shown in Fig. 4. It employs a copper-beryllium wire of 0.125 mm diameter, stretched inside the bore of the CLIC main beam quadrupole-BPM assembly. In this setup, the wire length is about 861 mm. The wire is supported independently from the magnet-BPM assembly by means of two marble-based support poles and a pretensioning system using a stepper motor, about whose shaft the wire is wound. Each wire end lays in between a couple of 0.1 mm diameter ceramic spheres. The repeatability in repositioning the wire using the support mechanics was analyzed, and the error is below $\pm 1.5 \mu\text{m}$ [14]. At both wire ends, two linear displacement stages from PI-miCos, mounted orthogonally, allow the wire to be

positioned and orientated with a repeatability better than $0.1 \mu\text{m}$, with an absolute accuracy better than $1.0 \mu\text{m}$, over a travel range of 50 mm. A signal generator excited wire vibration, required for the magnetic axis investigation, is measured by a set of optical micrometers from Keyence[®], orthogonally mounted on one of the wire translation stages, therefore following the wire position. These micrometers have a measurement range of 6 mm, a measurement repeatability of $\pm 0.03 \mu\text{m}$, and an accuracy of $\pm 0.5 \mu\text{m}$. They generate a voltage signal proportional to the wire displacement, which is then acquired by an 18-bit DAQ system from National Instruments[®]. A stable signal generator from Keithley[®] is used to excite the wire with an alternating current.

F. The nanopositioning system

The nanopositioning system utilized in the FPAB is shown in Fig. 3(a). It is based on previous studies for the CLIC stabilization system [15–17] and includes a new base [Fig. 3(b)] and lowered side plates to clear the line of sight for the fiducials located on the magnet for the micro-triangulation system. The magnet is placed on a network of four piezoelectric legs inclined by 20° with respect to the vertical plane. To maximize the stiffness in the transverse and roll degrees of freedom and to block the translational degree of freedom parallel to the beam line, 16 steel shear pins connecting the fix supporting frame and the magnet were included in the assembly.

The piezo stack actuators have a resolution of 0.15 nm and provide a maximal range of $15 \mu\text{m}$. A strain gauge sensor is embedded inside each actuator to measure their elongation. In addition, four incremental linear encoders are integrated in the assembly to measure directly the vertical and lateral displacement of the magnet with respect to its support frame. These displacements are measured at the front and the back of the magnet by rulers and vertical

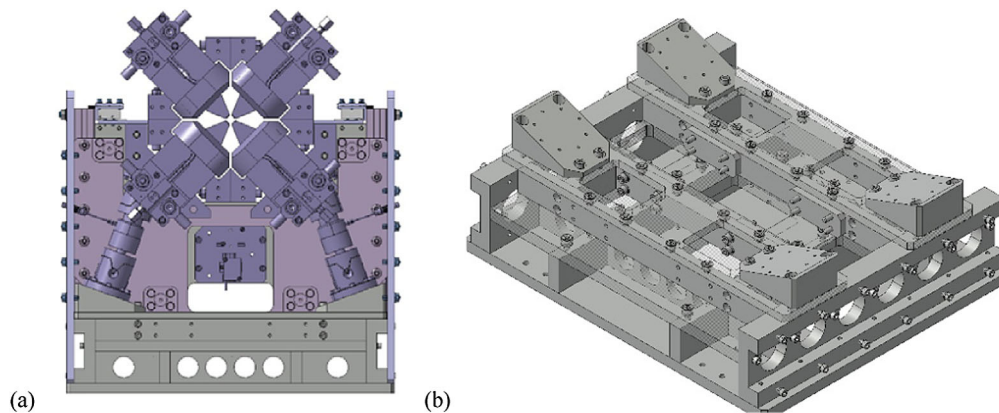


FIG. 3. (a) Front view of the nanopositioning system; the magnet rests on the inclined piezoelectric actuators. (b) The base needs to remain light but extremely stiff and consists of two plates connected by several transverse and longitudinal stiffener elements.

encoders. They provide 1 Vpp analog output signals, and their signal period is $0.512 \mu\text{m}$.

G. Alignment targets and stretched wire

Ceramic spheres are used as fiducial alignment targets. The spheres have a sphericity better than $1 \mu\text{m}$ (grade 40, ISO 3290) and diameters of 12.7 mm for the magnet and on the CMM granite table or 8 mm for the prealignment sensor kinematic mount. A small magnetic part has been glued on the ceramic spheres for an easier mounting on their magnetic support.

The copper-beryllium (CuBe) wire (98% and 2%) with a diameter of $125 \mu\text{m}$ and a form error of a few micrometers fulfils all the requirements to be used as a reference stretched wire for magnetic, electric, and metrological measurements [18]. Two different measuring systems were employed to determine the position of the fiducials and the wire, the Leitz Infinity CMM and the QDaedalus measuring system, based on theodolites equipped with a camera.

The Leitz Infinity CMM performs measurements to the fiducial points with various styli, depending on the accessibility of the targets: Contactless measurements to the wire are carried out with a PRECITEC LR Optical sensor. This sensor is a chromatic confocal sensor working in visible light with a measuring range of $100 \mu\text{m}$ and a measuring spot diameter of $3.5 \mu\text{m}$. It is an optical stylus with a diameter of 8 mm and a length of 66 mm, weighting 36 g.

The microtriangulation performs noncontact automated measurements of the wire and the fiducials. This QDaedalus measuring system was designed and developed primarily for astrogeodetic applications by the Geodesy and Geodynamics Lab, Institute of Geodesy and Photogrammetry, ETH Zurich. It consists of both software and hardware add-ons to a robotic theodolite. The fundamental idea is to replace the eye piece with a CCD camera in a nondestructive way, enabling automatic horizontal and vertical angle measurements to visible targets [19,20]. The angle measurements form a microtriangulation network which is a specific type of triangulation with two main features: it is optimized for short-range applications and employs high-accuracy industrial theodolites. These two features combined enable the measurement of fiducial coordinates with a precision in the order of a few micrometers.

III. ASSEMBLY AND PREPARATION OF THE SYSTEMS

The FPAB was assembled and installed in the CMM room, as shown in Fig. 4, for the fiducialization of the electromagnetic axes of the BPM and quadrupole. Robotic theodolites equipped with the QDaedalus measuring system were added to validate the concept of fiducialization utilizing the microtriangulation method.

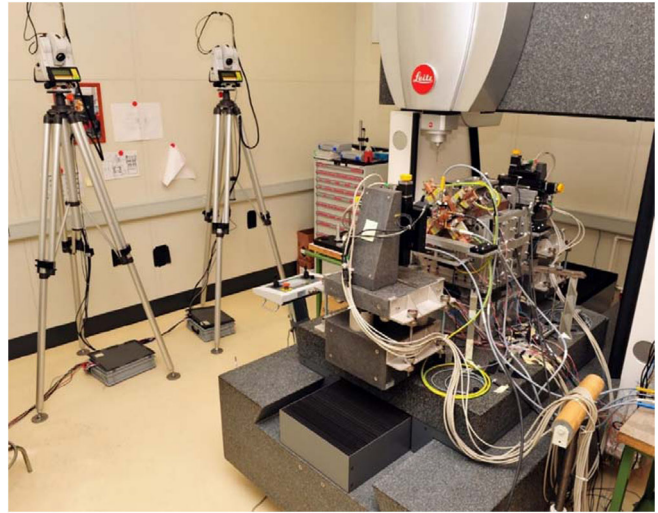


FIG. 4. View of the FPAB as finally assembled in the metrology lab. Two of the four microtriangulation network towers are also visible.

A. Mechanical alignment of components

The cavity BPM is directly mounted on the quadrupole core. In order to maximize the range of linear position dependency of the BPM, the reference axes of the BPM and quadrupole have to be aligned collinear and as close as possible to each other. Therefore, a specific strategy is followed, which ensures the assembly and alignment of the cavity BPM and quadrupole according to their mechanical axes. The BPM mechanical central axis was defined as the straight line, fixed by the measured central points of the two external flanges [see Fig. 5(a)]. The mechanical central axis of the quadrupole was instead defined as the axis passing through at the center of the four pole vertices measured at each magnet extremity [see Fig. 5(b)]. These measurements were performed with a portable measuring arm, equipped with a touching probe.

Two complementary precision parts were designed and manufactured to rigidly attach the BPM to the quadrupole. The one attached to the quadrupole [Fig. 6(a)] has three concentric ellipses which center the mechanical axis of the quadrupole; the other part interfaces the BPM through three pins, matching the slotted holes on the complementary part [Fig. 6(b)]. An exploded view of the assembly is shown in Fig. 6(c).

A cylindrical shaft was machined for alignment purposes. Passing through the MBQ, it was used to center the BPM. Misalignments were detected by means of a CMM and consequently adjusted. The resulting error of the matching between the two components is about $-52 \mu\text{m}$ for the horizontal and $27 \mu\text{m}$ for the vertical axes, with a parallelism of $70 \mu\text{m}$ [21].

Despite the fact that both MBQ and BPM are axisymmetric objects, there are non-negligible offset errors in the transverse directions; they can be mainly explained by two

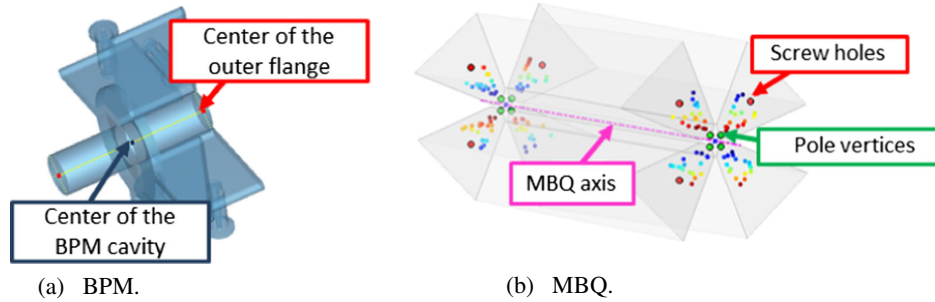


FIG. 5. (a) BPM and (b) MBQ magnet mechanical axis definition.

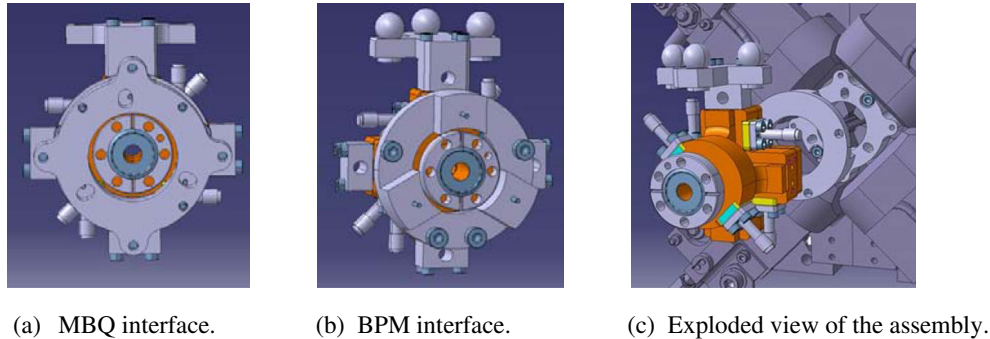


FIG. 6. 3D model views of the MBQ-BPM joints.

reasons:(i) on the MBQ side, the complementary mounted element refers to the four magnet poles that are affected by the precision of the four magnet quadrant assembly, and (ii) on the BPM side, the complementary mounted element is aligned with respect to the BPM external surface, since there is no access for metrology measurements to the BPM internal surface.

B. Preparation and sanity checks

Several sanity checks took place before performing the stretched-wire measurements of the entire assembly in the CMM environment.

1. Compatibility of the microtriangulation system in the CMM environment

The CMM measuring room is classified as class 1, according to the VDE/VDI 2627 standard. It operates in a reference temperature of 20°C and with temperature gradients of 0.2 K/h, 0.4 K/d, and 0.1 K/m. Four Leica TDA5005 were installed in the CMM room around the PACMAN test bench for the microtriangulation measurement. The Leica AT21 aluminum tripods were fully extended, and all the instruments had a similar height of about 2.3 m above the floor. The temperature variation combined with the tripod length and the material (aluminum) was expected to cause a height variation of the

theodolites which could be observed as vertical angle variation.

A test measurement was performed to measure the angle variation. The four theodolites observed a stable target (ceramic sphere) on top of the assembly, and the horizontal and vertical angles were recorded for about 1.5 h [Fig. 7(b)]. According to the manufacturer specifications, the angular accuracy of these theodolites is 0.15 mgon \approx 2.4 μ rad or 2.4 μ m/m (1 σ , ISO17123-3).

Simultaneously, the temperature variation of the four temperature sensors, mounted on the CMM, was recorded [Fig. 7(a)]. The mean value of the four temperature sensors was used to estimate the vertical angle variation, under the assumptions that the expansion of the tripod legs mainly affects the height of the instruments and the expansion of the aluminum legs is linear with a coefficient of 23 μ m/°C/m. For the calculations, the geometry of the station number 3 (STA3) and the target (MAG) was used.

In Fig. 7(b), we show the results of the variation of the vertical angle, demonstrating a good agreement between the measurement and estimation. The variation is significant with respect to the intrinsic precision of the theodolites. Various techniques could be used to correct this effect, such as modeling this systematic error. In our case, for the microtriangulation network, we significantly reduced the acquisition time to about 10 min for one network and repeated the network measurement for more than an hour in order to mitigate the error by averaging the data over time.

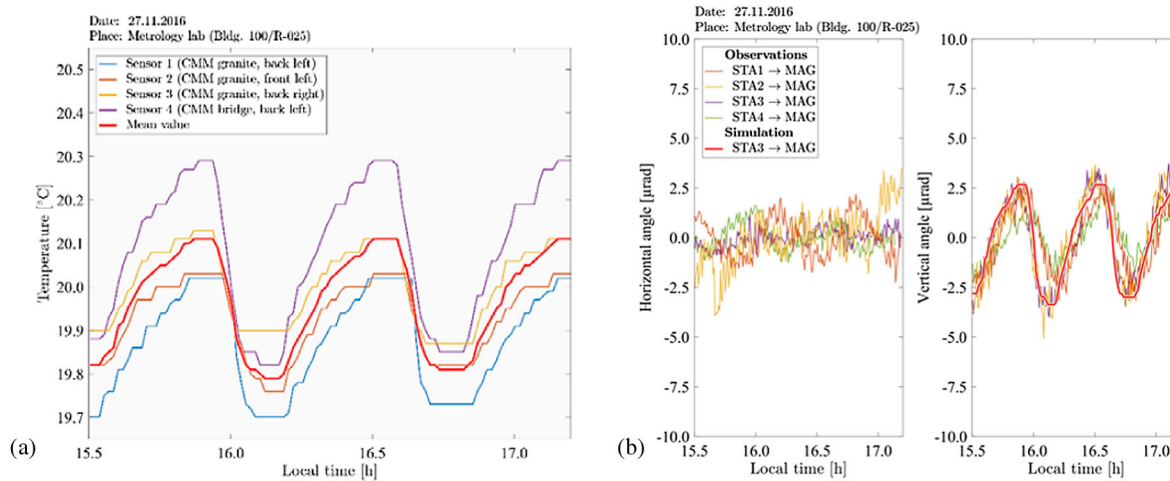


FIG. 7. (a) Temperature variation and mean value as measured by four sensors mounted on the CMM. (b) Horizontal and vertical angle observations from four theodolites to a target on top of the magnet. The red line depicts the simulated vertical angle variation according to the temperature variation and the geometrical configuration.

2. Impact of the magnet current on the position of the magnetic axis

One of the concerns for the stretched-wire characterization of the main beam quadrupole axis was on excessive heating sources inside the well-stabilized thermal environment of the CMM. To minimize unwanted thermal effects on the measuring environment, the magnet was powered well below its nominal current (4 A against 126 A), avoiding the necessity of a cooling system whose operation would have been altering the thermal conditions of the room. On the other hand, the low excitation of the magnet substantially reduces the field intensity (about 2.7 T integrated gradient compared to the nominal 70 T [22]), which increases the influence of background magnetic fields [23]. To correct for this effect, measurements with alternating current polarities (4 and -4 A) were taken, with the results averaged. Table II lists the discrepancy of the magnetic axis found using this method, compared with the standard measurement procedure at the nominal excitation current.

TABLE II. Offset between the magnetic axis at 4 and 126 A.

Horiz. center	Vert. center	Yaw	Pitch
2.9 μm	3.1 μm	$-2.3 \mu\text{rad}$	$-5.1 \mu\text{rad}$

TABLE III. Offset between the mechanical axis and the magnetic axis at 126 A.

Horiz. center	Vert. center	Yaw	Pitch
32.2 μm	20.2 μm	$-75.9 \mu\text{rad}$	$-57.4 \mu\text{rad}$

3. Offset between magnetic and mechanical axes of the quadrupole

A geometric survey was performed to measure the offset between the magnetic and the mechanical axis of the quadrupole. A measuring arm and a laser tracker were used for this measurement. The measuring arm detected the pole tips of the magnet on each side and the fiducial points on the magnet, while the laser tracker measured the fiducial points on the magnet and points at both ends of the wire. The independent point clouds were fitted together by 3D transformations, based on the common points. The 3D adjustment of the point cloud had uncertainty in the level of 15 μm . Subsequently, the mechanical axis was calculated and compared with the magnetic axis as measured at the nominal current (126 A). The offset between the two axes is presented in Table III.

IV. MEASUREMENTS AND ANALYSIS OF THE RESULTS

A. Magnetic axis

The vibrating-wire method was chosen to locate the magnetic axis, because of its high sensitivity also at a low magnetic field excitation of the quadrupole magnet. This method is based on the conductive CuBe wire being stretched through the magnet and fed with a sinusoidal current signal, such that the interaction of the current with the magnetic field causes a wire “vibration” with a frequency matching one of the mechanical eigenmodes of the wire. The vibration amplitude in the steady state is proportional to the magnetic field. The measured transfer function $F(\omega)$ is the product of the wire vibration and current averaged over a period $T = 2\pi/\omega$. As the magnetic field in a quadrupole grows proportionally with the distance from the axis, the magnetic axis is found by the linear

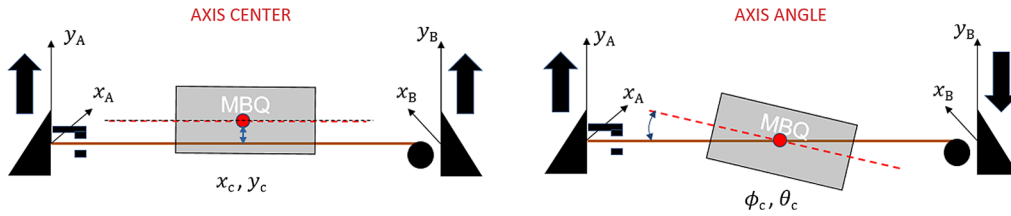


FIG. 8. Magnetic axis coordinate definition in the local reference frame of the wire stages.

interpolation of the measurement function values and extrapolation of the location where F would be zero. The drive-current frequency is chosen such that it matches the resonance of the wire eigenmode and, thus, increases the measurement sensitivity. Furthermore, by positioning the magnet at the vibration antinode of the fundamental mode (corresponding to the node of the second mode), the alignment results are decoupled for positions and angles: (i) wire codirectional movement and first resonant mode excitation for the horizontal x_c and vertical y_c magnetic centers, and (ii) counterdirectional movement and second resonant mode for the yaw φ_c and pitch θ_c angles. The coordinates of the magnetic axis in the local reference frame of the wire stages are depicted in Fig. 8.

To determine the magnetic axis in the local reference frame, a vibrating-wire scan was performed for each coordinate: (i) horizontal codirectional scan for x_c , (ii) vertical codirectional scan for y_c , (iii) horizontal counterdirectional (yaw) scan for φ_c , and (iv) vertical counterdirectional (pitch) scan for θ_c .

The same was repeated with the magnet excited at both 4 and -4 A. The measured values of the F function for each scan with the interpolation traces and the extracted magnetic axis coordinates are shown in Fig. 9. The displacements (x, y, φ, θ) are given with respect to the wire initial position. The F function values are given as readout voltage from the Keyence optical sensors per unit of wire drive current. The final set of coordinates was

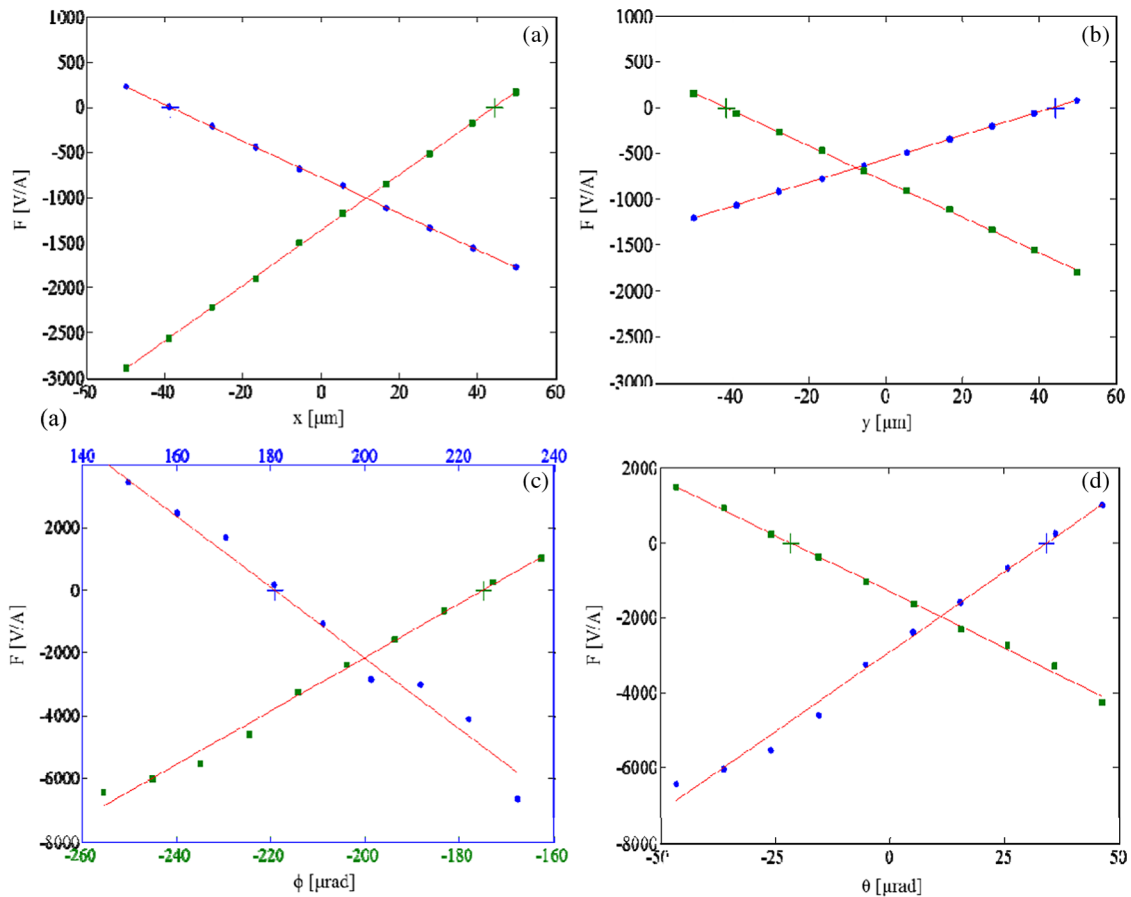


FIG. 9. Vibrating-wire measurement results for the localization of the magnetic axis. Blue circles: measurements at 4 A magnet excitation current; green squares: measurements at -4 A excitation. (a) Horizontal codirectional scan. (b) Vertical codirectional scan. (c) Horizontal counterdirectional scan. (d) Vertical counterdirectional scan.

TABLE IV. Repeatability of the magnetic axis measurement.

σ_x	σ_y	σ_φ	σ_θ
$\pm 0.06 \mu\text{m}$	$\pm 0.08 \mu\text{m}$	$\pm 1.94 \mu\text{rad}$	$\pm 0.41 \mu\text{rad}$

determined by averaging the results obtained at 4 and -4 A. The repeatability of each wire scanning was assessed as the 1σ standard deviation on a sample of ten repetitions, obtaining the values listed in Table IV. The wire sagitta at the middle point was estimated by the measurement of the wire fundamental frequency ω_1 and the formula (1) [7] ($g = 9.81 \text{ m/s}^2$), resulting in a wire sag of $9 \mu\text{m}$:

$$s = \frac{g}{32} \left(\frac{2\pi}{\omega_1} \right)^2. \quad (1)$$

The results demonstrate the effectiveness of the adopted method to locate the magnetic axis at a reduced magnet excitation current with a repeatability within $\pm 0.1 \mu\text{m}$, measured at the magnet edge (Table IV). Effects from background magnetic fields could be adequately corrected; furthermore, the error from the wire sagitta was estimated and corrected. Once the magnetic axis was determined, the wire was replaced at the predicted position using the lateral stages for its localization in the external reference frame of the CMM. In a future measurement campaign, the measurement reproducibility will be investigated.

B. Electrical axis

A first characterization of the cavity BPM was performed on a dedicated test bench in a laboratory environment. This allowed the study of the best rf measurement method. The conductive wire was simply stretched through the cavity and fixed on both ends. A relative motion between the wire and position cavity was performed through translation stages, able to move with submicrometric resolution in a range of a few millimeters. The wire represents a perturbation for the electromagnetic fields of the excited dipole eigenmode of the cavity, which is minimum when the wire is located in the electrical center. For the rf measurements, the BPM was considered as a four-port device under test, with the ports corresponding to the four lateral waveguides. They are originally used as signal pickups and now serve as rf ports for scattering parameter measurements, acquired with a commercial vector network analyzer at each wire displacement step. The most valuable information was found to be the analysis of the phase of the S parameter transmission between adjacent ports (e.g., $\angle S_{41}$, exciting from port 1 and reading the signal out from port 4). We can detect the electrical center coordinate by observing the phase transition related to the wire crossing the electrical center axis. By performing a sweep of the wire parallel to the two transverse coordinates (x, y) (x for radial direction

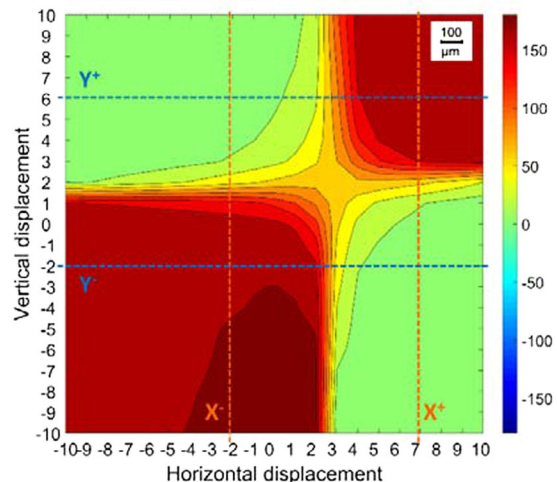


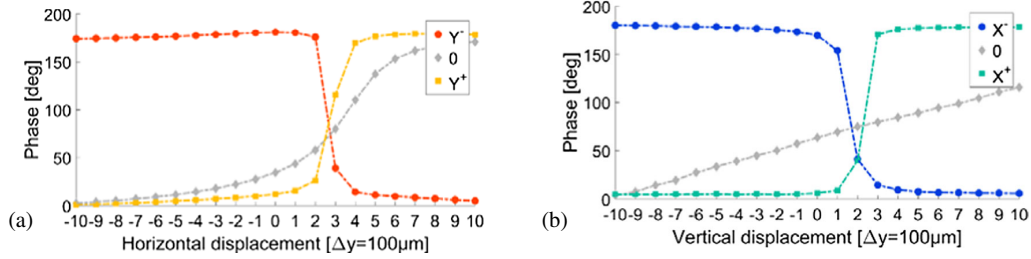
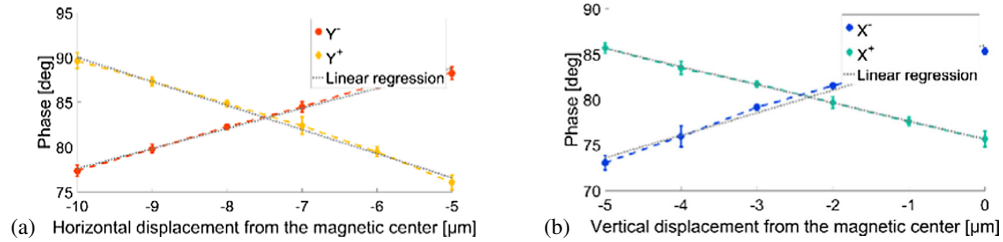
FIG. 10. S41 parameter pattern resulting from a 2D position sweep between the wire and BPM.

and y for the vertical direction), we found the contours of the measured phase, e.g., $\angle S_{41}$, are divided in four sectors, assessing a 180-degree phase transition, which corresponds to the wire crossing the electrical center, as displayed in Fig. 10 [24].

Moving the wire along two paths parallel to the transverse coordinates and symmetric to the electrical center, as indicated, e.g., $Y+$ and $Y-$, we measure two symmetric phase responses (see Fig. 10). The intersection of the traces identifies the change of the polarity of the electric field and, therefore, the corresponding coordinate value of the electrical center of the BPM. As Fig. 11 indicates, the procedure needs to be repeated to acquire the values of both coordinates of the electrical center. The position information is returned by the feedback circuit of the translation stages and is referenced to the previously identified magnetic axis of the quadrupole (see Sec. IV A) and, thus, is a direct measurement of the offset between the magnetic center of the quadrupole and the electromagnetic center of the cavity BPM.

The results shown in Fig. 12 are obtained by performing a position sweep of the wire over a smaller range, with a step size of the translation stages of $1 \mu\text{m}$. The electromagnetic alignment between the two devices is found to be in the micrometric range: about $-2.3 \mu\text{m}$ on the horizontal axis and $-7.5 \mu\text{m}$ on the vertical one. Moreover, the measurements were repeated several times with the FPAB being located in the CMM room under stable and temperature-controlled conditions, demonstrating submicrometric repeatability.

As a summary, the repeatability in the determination of the magnetic axis of a quadrupole using a stretched wire and of the electrical center of a BPM is very satisfactory, below $1 \mu\text{m}$. The reference axis of both components is not so close from the mechanical axis, despite the very good tolerances of manufacturing of the components and of the

FIG. 11. (a) Vertical and (b) horizontal coordinate of the electrical center located through S41 observation, $\Delta = 50 \mu\text{m}$.FIG. 12. (a) Vertical and (b) horizontal coordinate of the electrical center located through S41 observation, $\Delta = 1 \mu\text{m}$.

methods developed for the assembly: more than $40 \mu\text{m}$ in vertical in both cases (see Table V). The offsets between the BPM and quadrupole axes are known within a micrometric accuracy with the methods of measurements developed.

C. Microtriangulation vs CMM measurements

During the PACMAN measurement campaign, the CMM performed a metrology measurement to be used as a reference for comparison with the microtriangulation method. The preliminary results presented here attempt to evaluate the location of the wire and the quadrupole-BPM fiducials in absolute coordinates, based on the two different measurement algorithms, as well as a novel geodetic network solution which combines points and lines of the acquired metrology data based on a least-squares analysis. Both algorithms were developed in the PACMAN project.

The measurements consist of three parts: (i) a series of ten microtriangulation measurements using the QDaedalus system (1st period), (ii) Leitz Infinity tactile measurements to the fiducials and contactless measurements to the stretched wire, and (iii) a series of nine microtriangulation

TABLE V. Mechanical, magnetic, and electric axes center offset.

	X [μm]	Y [μm]	Uncertainty [μm]
MBQ (magnetic vs mechanical)	-21.6	40.9	± 10
BPM (electric vs mechanical)	17.3	40.6	± 4
BPM/MBQ (electric vs magnetic)	-2.3	-7.5	± 1.2

measurements, again using the QDaedalus system (2nd period).

In each of the 19 microtriangulation measurements, 20 fiducials fixed on the quadrupole magnet and the cavity BPM, as well as the stretched wire, were measured in two circles (left circle and right circle) by four theodolites. Each series was completed in about 11 min, and each of the two measurement sessions took about 2 h. The CMM measurement was completed in about 6.5 h.

The comparison of the acquired metrology data was performed for the position of the fiducials and the position and orientation of the wire in space. Because of the fact that the two coordinate systems—that of the microtriangulation and that of the CMM—are not parallel, we applied a 3D Helmert transformation in order to compare the data. The average of the 19 measurement series was transformed to the CMM coordinate system. The differences of the fiducial points as measured by the CMM and by the QDaedalus are depicted in Fig. 13. The differences demonstrate the accuracy of the microtriangulation method compared to the accuracy of the CMM, which is about $12 \mu\text{m}$. In Fig. 13, we can see the statistics of the differences, expressed as 3D vectors.

For the fiducial targets, 85% of the measured differences of the absolute coordinate values were smaller than $15 \mu\text{m}$, 75% were smaller than $10 \mu\text{m}$, and about 42% were found to have absolute differences smaller than $5 \mu\text{m}$. Higher difference values appear in the lateral direction to the wire axis due to the poor geometry of the network. For the wire position, we observed a difference between the microtriangulation and the CMM measurement in the mean point of the wire of $27 \mu\text{m}$ in the Y axis (lateral to the wire) and

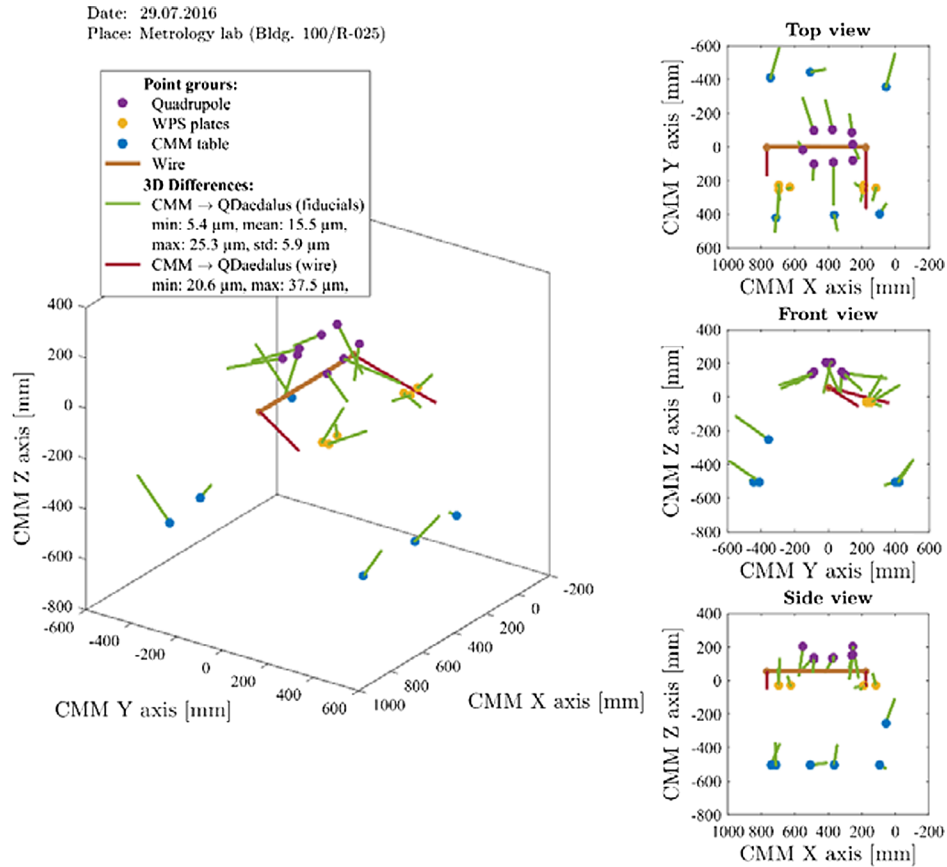


FIG. 13. Differences in the results of fiducialization between the CMM and microtriangulation.

about 10 μm in the Z (vertical) axis. For the wire orientation, the difference between the microtriangulation and the CMM measurement was 32 $\mu\text{m}/\text{m}$ in the lateral direction and about 3 $\mu\text{m}/\text{m}$ in the vertical direction.

D. Nanopositioning measurements

We carried out two experiments using the nanopositioning system. The objective of the first experiment was to assess the accuracy of the trajectory of the magnet for a nominal vertical displacement, comparing the result to the CMM measurements. A 7.5 μm square displacement signal was applied to the magnet, and the same pilot signal was sent to all the piezoactuators. The magnet displacement was measured by the CMM (via the coordinates of the fiducials glued on top of the magnet) and the sensors embedded into the nanopositioning system (strain gauge sensors and incremental linear encoders).

By comparison to the CMM measurement of the repeated displacement steps, the accuracy of the nanopositioning system was found to be at least as good as the limit of the uncertainty of measurement of the CMM. In addition, the maximal parasitic lateral displacement measured by the CMM was 1 μm . The maximum parasitic rotations measured were 1.7 μrad in pitch and 1.3 μrad in yaw.

The objective of the second experiment was to cross-check the mechanical displacement applied to the magnet and the magnetic axis displacement measured via the vibrating stretched-wire technique. For this test, a fixed displacement step of 2 μm was applied sequentially four times to the magnet in the vertical direction, again using the same pilot signal for all piezoactuators. The nominal magnet positions were then 0, 2, 4, 6, and 8 μm . The magnet positions were measured by the same set of sensors (CMM, strain gauge sensors, and encoders). Furthermore, a magnetic measurement was performed at each step: the magnetic axis positions were detected based on the vibrating stretched-wire system.

Considering all steps, the offset between the vibrating stretched-wire system and all the other sensors was below 0.7 μm . This confirms the relative accuracy of the vibrating-wire system below one micron for the localization of the magnetic axis of the quadrupole magnet.

V. PERSPECTIVES

A. An absolute fiducialization of accelerator components in the micrometric regime

Measurements using a stretched wire to locate the reference axis of components were already carried out at

SLAC using a 3D coordinate measuring machine [7]. The SLAC CMM measured the positions of the fiducials on quadrupoles with respect to wire position detectors with a repeatability of $15\ \mu\text{m}$, but there were no direct measurements of the position of the wire.

PACMAN added the direct measurement of the reference axes of each component with respect to their sensor fiducials, enabling a straightforward way to align the component during the installation in the tunnel. In the CLIC conceptual design report, a strategy of prealignment has been proposed to fulfil the alignment requirements summarized hereafter. Alignment systems (wire or laser based) with a length of more than 200 m will be installed all along the tunnel to provide a straight and accurate reference to position the components. After transportation in the tunnel, each component or support assembly will be located coarsely in its place. Then, prealignment sensors plugged on the component or on its support assembly will perform radial and vertical offset measurements with respect to the alignment references. Combining these sensor prealignment measurements and the fiducialization measurements performed in the CMM, one can determine the position of the reference axis of the component (or support assembly) with respect to the alignment reference at a micrometric accuracy, relating different coordinate systems.

During the PACMAN fiducialization process, both the position of the component reference axis and the position of the prealignment sensor supporting system are determined by CMM measurements in the component coordinate system. Each prealignment sensor is equipped with a mechanical interface allowing its micrometric repositioning on the component or support assembly. On top of this, each prealignment sensor has been calibrated in such a way that the position of the alignment reference is known within an accuracy of $5\ \mu\text{m}$ and a repeatability of $1\ \mu\text{m}$ in the mechanical interface coordinate system.

As a consequence, the position of the component reference axis with respect to the straight tunnel alignment reference is known within a micrometric error budget, considering (i) the repeatability of the determination of the reference axes of quadrupoles and BPM using a stretched wire: $1\ \mu\text{m}$, (ii) the uncertainty of measurement of the CMM for the combined measurements of the wire (noncontact probe) and the reference spheres (tactile measurements): $2\ \mu\text{m}$, (iii) the repeatability of the mounting of the prealignment sensor on top of its kinematic mount: $1\ \mu\text{m}$, and (iv) the accuracy of the measurement of the sensor: $5\ \mu\text{m}$.

These errors, originating from different measurement sources, are independent, and a first estimate of the budget of error can be given as the square root of the sum of the squared errors. As a first estimate, the error budget is $5.6\ \mu\text{m}$ assuming no environmental effects, e.g., temperature drifts.

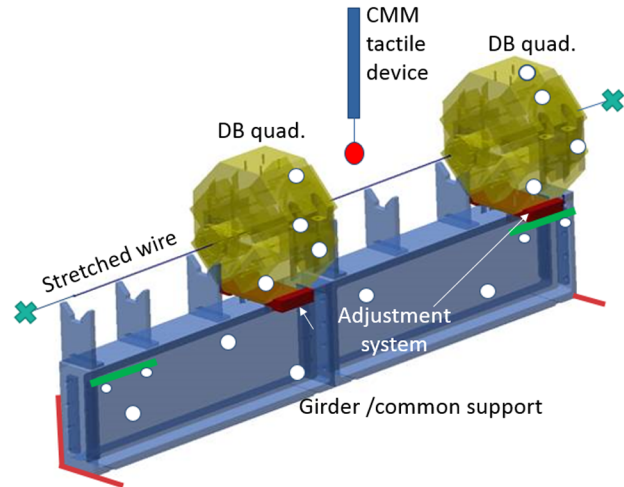


FIG. 14. Fiducialization and initial alignment of DB quadrupoles.

B. A micrometric alignment of accelerator components on the same support assembly

The PACMAN fiducialization process improves the accuracy of fiducialization and can be applied to several components at the same time, using the same stretched wire to gain accuracy and relax manufacturing tolerances on the support assembly of the components. In the CLIC conceptual design report, two drive beam (DB) quadrupoles will have to be aligned on a single girder support; the error budget between their reference axes and a straight reference alignment in the tunnel is $20\ \mu\text{m}$ at 1σ . First tests have been performed on real size components using mechanical shims in order to align the DB quadrupoles in the coordinate system of the girder. Substantial periods of time (many hours) were required to adjust the quadrupoles in 5 degrees of freedom to the nominal position [25]. To provide more flexibility, dedicated 5 degrees of freedom adjustment systems were developed specifically to replace the time-consuming shimming. They are based on a combination of three flexible wedges, adjustable by knobs at a micrometric resolution and specific threads for the radial translations [26]. After the installation of the two 5 degrees of freedom adjustment systems on the girder, the DB quadrupoles can be put in place. In the CMM environment, a wire is stretched through the quadrupoles. Acting on the adjustment systems, using the oscillating wire method, the two reference axes would be aligned to their nominal position. The position of the stretched wire is then measured with respect to the fiducials of the quadrupoles and with respect to the prealignment kinematic mount of the sensors. Such a procedure would perform with an estimated accuracy of a few micrometers (see Fig. 14). It can be extrapolated to the other accelerator components like BPMs and rf structures.

C. A portable alternative to CMM measurements

As mentioned before, a portable alternative to the CMM measurements is under development. CMM measurements

are the most accurate measurements that can be performed to measure an object but also have drawbacks: the limited measurement volume (in the case of the Leitz Infinity CMM, its major axis stroke is 1.2 m) and the fact that a CMM is static and cannot be transported and used in the accelerator tunnel. The combination of microtriangulation and FSI measurements will propose a portable alternative to CMM measurements, with an accuracy of measurements below $5\ \mu\text{m}$. The combination of two different measurement methods is very valuable, as it offers redundant measurements from systems based on different measurement principles (one performing absolute distance measurements based on frequency scanning interferometry, the other performing remote angle measurements). Thanks to this combination of measurement systems, fiducialization and initial alignment could be performed directly in the tunnel, probably in a dedicated area. Such a portable combination of metrology measurement systems will offer the possibility to verify the correct alignment of the components to their support structure or assembly, in the tunnel, before or after their final installation. They also could be used also in the case of a change of a component in the tunnel.

VI. CONCLUSION

The PACMAN project proposes a new solution to fiducialize the reference axes of accelerator components, using a stretched wire. Methods to locate the magnetic axis of a quadrupole and the electromagnetic zero of a BPM have been successfully demonstrated. A prototype assembly of a CLIC main beam quadrupole and a 15 GHz cavity BPM was used to quantify the developed alignment methods in a CMM environment, demonstrating submicrometric repeatability of the measurements for both components. The reproducibility of the measurements for both methods remains to be validated. Furthermore, a microtriangulation method based on angle measurements is proposed as an alternative to CMM measurements: It was developed and validated, allowing the measurement of the position of the wire with respect to external fiducials and prealignment sensor interfaces. First results compared with CMM measurements are promising.

The presented new methods for the fiducialization reduce measurement time while improving accuracy for the alignment of accelerator components. It can be applied to components with length dimensions short enough to be measured by a CMM, with micrometric requirements of prealignment. The concept was validated on CLIC components, including rf structures not detailed in this paper, and could be applied to future projects like FCC-ee, where prealignment requirements are equivalent.

ACKNOWLEDGMENTS

The research leading to these results has received funding from the European Union's 7th Framework Program Marie Curie actions, Grant Agreement No. PITN-GA-2013-606839.

- [1] S. Griffet *et al.*, Report No. CERN-ATS-2012-079.
- [2] M. Aicheler *et al.*, Report No. CERN-2012-007.
- [3] N. Catalan Lasheras *et al.*, Measuring and aligning accelerator components to the nanometre scale, in *Proceedings of the 5th International Particle Accelerator Conference, Dresden, Germany, 2014* (JACoW, Shanghai, China, 2014).
- [4] H. Mainaud Durand *et al.*, Status of PACMAN project, in *Proceedings of IBIC 2015, Melbourne, Australia* (JACoW, CERN, Switzerland, 2015).
- [5] D. Noelle, BPMs with precise alignment for TTF2, *AIP Conf. Proc.* **732**, 166 (2004).
- [6] H. Mainaud Durand *et al.*, Theoretical and practical feasibility demonstration of a micrometric remotely controlled pre-alignment system for the CLIC linear collider, in *Proceedings of the 2nd International Particle Accelerator Conference, San Sebastián, Spain* (EPS-AG, Spain, 2011), CERN-ATS-2011-082, CLIC-Note-090.
- [7] Z. Wolf, Report No. LCL-TN-05, 2005.
- [8] R. Ruland, Report No. SLAC-PUB-11424, SLAC, 1993.
- [9] S. Griffet, EDMS Report No. 1096102, CERN, 2010, <https://edms.cern.ch/document/1096102/1>.
- [10] N. Galindo Munoz *et al.*, Pre-alignment of accelerating structures for compact acceleration and high gradient using in-situ radiofrequency methods, in *Proceedings of the 7th International Particle Accelerator Conference, Busan, Korea* (JACoW, CERN, Switzerland, 2016).
- [11] M. Modena *et al.*, Performances of the main beam quadrupole type1 prototypes for CLIC, *IEEE Trans. Appl. Supercond.* **24**, 4002504 (2014).
- [12] F. Cullinany *et al.*, A prototype cavity beam position monitor for the CLIC main beam, in *Proceedings of the 1st International Beam Instrumentation Conference, Tsukuba, Japan, 2012* (JACoW, Geneva, Switzerland, 2012), pp. 1–3.
- [13] J. R. Towler *et al.*, Development and test of high resolution cavity BPMs for the CLIC main beam linac, in *Proceedings of the 4th International Beam Instrumentation Conference, Melbourne, Australia, 2015* (JACoW, CERN, Switzerland, 2015), pp. 1–5.
- [14] D. Glaude, CERN Technical Report No. EDMS 1532615.
- [15] S. Janssens, Ph.D. thesis, CERN/NIKHEF, 2015.
- [16] D. Ziemianski and M. Guinchard, Technical Report No. EDMS 1427645.
- [17] M. Esposito *et al.*, Development of advanced mechanical systems for stabilisation and nano-positioning of CLIC Main Beam quadrupoles, in *Proceedings of IWAA 2012, Fermilab, Chicago, Stanford University*, edited by R. Ruland, eConf. C1209102 (2012).
- [18] C. Sanz *et al.*, Report No. CERN-ACC-2015-0075.
- [19] S. Guillaume, B. Bürki, S. Griffet, and H. Mainaud Durand, QDaedalus: a versatile usable digital cli-on measuring system for total stations, in *Proceedings of FIG'12, Rome, Italy, 2012* (FIG, Copenhagen, Denmark, 2012).
- [20] B. Bürki, S. Guillaume, P. Sorber, and H. Oesch, DAEDALUS: a versatile usable digital cli-on measuring system for total stations, in *Proceedings of IPIN'10, Zurich, Switzerland* (IPIN, Guimaraes, Portugal, 2010).

- [21] S. Zorzetti *et al.*, Study of the electrical center of a resonant cavity Beam Position Monitor (RF-BPM) and its integration with the Main Beam quadrupole for alignment purposes, in *Proceedings of the 2016 North American Particle Accelerator Conference, Chicago, Illinois* (JACoW, CERN, Switzerland, 2016).
- [22] P. Arpaia, D. Caiazza, C. Petrone, and S. Russenschuck, Performance of the stretched- and vibrating- wire techniques and corrections of background fields in locating quadrupole magnetic axes, in *Proceedings of the XXI IMEKO World Congress, 2015, Prague, Czech Republic* (International measurement confederation (IMEKO), Budapest, Hungary, 2015).
- [23] A. B. Temnykh, Vibrating wire field-measuring technique, *Nucl. Instrum. Methods Phys. Res., Sect. A*, **399**, 185 (1997).
- [24] S. Zorzetti, Ph.D. dissertation, University of Pisa, Pisa, Italy, 2016.
- [25] H. Mainaud Durand *et al.*, Report No. CERN-ATS-2012-272, 2012.
- [26] H. Mainaud Durand *et al.*, Report No. CERN-ACC-2015-0083, 2014.